
BIOBRIDGE: BRIDGING BIOMEDICAL FOUNDATION MODELS VIA KNOWLEDGE GRAPHS

Zifeng Wang *

Department of Computer Science
University of Illinois Urbana-Champaign
zifengw2@illinois.edu

Zichen Wang

Amazon AWS AI
zichewan@amazon.com

Balasubramaniam Srinivasan

Amazon AWS AI
srbalasu@amazon.com

Vassilis N. Ioannidis

Amazon Search
ivasilei@amazon.com

Huzefa Rangwala

Amazon AWS AI
rhuzeafa@amazon.com

Rishita Anubhai

Amazon AWS AI
ranubhai@amazon.com

ABSTRACT

Foundation models (FMs) are able to leverage large volumes of unlabeled data to demonstrate superior performance across a wide range of tasks. However, FMs developed for biomedical domains have largely remained unimodal, i.e., independently trained and used for tasks on protein sequences alone, small molecule structures alone, or clinical data alone. To overcome this limitation of biomedical FMs, we present BioBRIDGE, a novel parameter-efficient learning framework, to bridge independently trained unimodal FMs to establish multimodal behavior. BioBRIDGE achieves it by utilizing Knowledge Graphs (KG) to learn transformations between one unimodal FM and another without fine-tuning any underlying unimodal FMs. Our empirical results demonstrate that BioBRIDGE can beat the best baseline KG embedding methods (on average by $\sim 76.3\%$) in cross-modal retrieval tasks. We also identify BioBRIDGE demonstrates out-of-domain generalization ability by extrapolating to unseen modalities or relations. Additionally, we also show that BioBRIDGE presents itself as a general-purpose retriever that can aid biomedical multimodal question answering as well as enhance the guided generation of novel drugs.

1 INTRODUCTION

Foundation models (Bommasani et al., 2021) trained on large volumes of data can be leveraged and adapted for different domains. In biomedicine, FMs are trained to ingest large volumes of text corpora (Gu et al., 2021) from scientific literature, protein data in the form of sequences and 3D-structures (Jumper et al., 2021), molecule data in the form of graphs and SMILES strings (Fabian et al., 2020) and protein-interaction data in the form of relational graphs. These pre-trained biomedical FMs have achieved a significant gain in comparison to previous methods trained on smaller datasets (Qiu et al., 2023).

Introducing multimodal data in training further boosts the performance of FMs, especially in few-shot/zero-shot prediction settings (Radford et al., 2021). In the biomedical domain, for drug-text (Edwards et al., 2022), protein-text (Liu et al., 2023), and drug-protein data (Huang et al., 2021; Ioannidis et al., 2020), multimodal data was leveraged by the joint optimization of unimodal encoders. However, this idea encounters key issues when scaling beyond two modalities:

*This work was completed while the author was an intern at Amazon.

- **Computational Cost.** These approaches require many unimodal encoders with approximately similar sizes to avoid impeding each other. This setup can cause a size explosion of the bundled models in a magnitude of the number of modalities, thus rendering a computational burden for performing joint optimization.
- **Data Scarcity.** They require pairwise cross-modal datasets of similar size to ensure stable training. The dataset quantity increases exponentially in a combinatorial order of $\binom{K}{2}$ where K represents the number of modalities, inevitably leading to data scarcity.

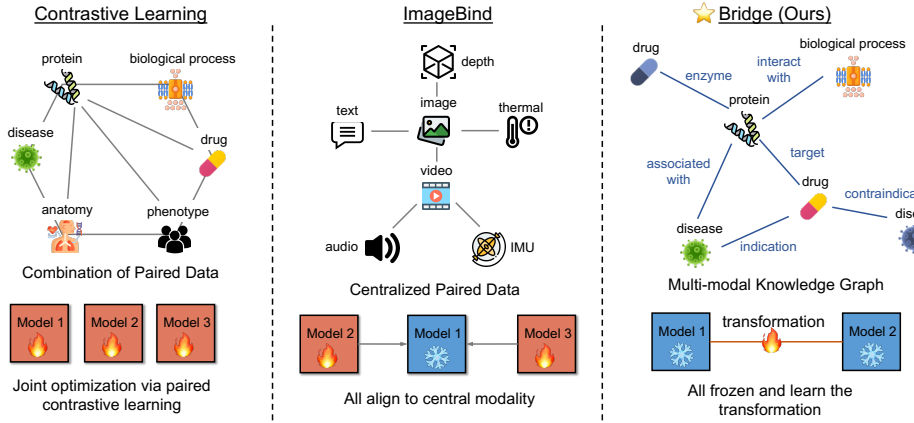


Figure 1: The conceptual comparison between our methods and previous methods. **Left:** multimodal contrastive learning, e.g., CLIP, learns from a combination of paired data, updating all unimodal encoders; **Middle:** ImageBind aligns all modalities with the central modality, with only the central model frozen; **Right:** BioBRIDGE learns the transformation across modalities from a multi-modal KG, keeping all FMs frozen.

Unlike ImageBind (Girdhar et al., 2023), which sets the image as the central modality and aligns all the other encoders with the image via fine-tuning, the proposed BioBRIDGE keeps all the unimodal FMs fixed and learns to bridge these unimodal FMs. The conceptual demonstration is shown in Figure 1. Specifically, BioBRIDGE learns the cross-modality transformation from biomedical knowledge graphs (KGs). This approach is modeled by leveraging the following insights:

- **Data Sufficiency.** It is usually easier to collect unimodal data than to collect paired data from two modalities. For instance, close to 250M protein sequences (Rives et al., 2021) and 1.5B molecule structures (Sterling & Irwin, 2015) are available to perform self-supervised pre-training, while only 441K protein-text pairs are one of the largest of biological multimodal datasets (Liu et al., 2023). As such, compared to the joint training of multimodal encoders, bridging independent models that were trained on unimodal data at scale enjoys the merits of data sufficiency and efficiency.
- **Structural Transformation.** Multimodal biomedical KG contains the structure information represented by the triplets of head and tail biomedical entities and their relationships. It covers a rich set of modalities such as protein, molecule, and disease (Chandak et al., 2023), which enables comprehensive biomedical analytics and ML. We align the embedding space of unimodal FMs through a cross-modal transformation model utilizing the rich structure in KG triplets.

In summary, the proposed BioBRIDGE aims to create a universal bridging mechanism capable of efficiently connecting the representations of any pairs of modalities. Technically, the bridge modules are supervised by the rich structure information from knowledge graphs, while the unimodal FMs are kept frozen to advance the parameter and computation efficiency. Experimental evaluation shows that:

- The bridged unimodal FMs are competitive in diverse cross-modal prediction tasks.
- BioBRIDGE can extrapolate to nodes that are not present in the training KG with comparable performance as the supervised baselines.

- BioBRIDGE generalizes to relationships that do not exist in the training KG, and the performance can be enhanced with further training.

2 RELATED WORK

Foundation Models. The discovery of foundation models has sparked remarkable breakthroughs (Bommasani et al., 2021) across a diverse spectrum of fields such as natural language processing (Brown et al., 2020), computer vision (Kirillov et al., 2023) and others. In biomedicine, FMs are trained with masked language modeling for text (Gu et al., 2021), proteins (Rives et al., 2021; Lin et al., 2023), drug molecules (Wang et al., 2019a), or with generative modeling for text (Taylor et al., 2022), protein (Madani et al., 2023), molecule (Bagal et al., 2021). These FMs usually trained on one data modality are used as feature extractors in supervised prediction tasks such as protein-protein interaction (Wang et al., 2019b; Hallee & Glehorn, 2023), protein function prediction (Gligorijević et al., 2021; Wang et al., 2022a) and drug-target interaction (Sledzieski et al., 2022; Kalakoti et al., 2022).

In the literature, multimodal biomedical FMs leverage contrastive learning on the pairs of image-text (Wang et al., 2022b), drug-protein (Huang et al., 2021), drug-text (Edwards et al., 2022) and protein-text (Liu et al., 2023; Xu et al., 2023). Nonetheless, extending these approaches beyond two modalities is challenging due to the need of large volumes of pairs of multimodal datasets. A recent effort (Girdhar et al., 2023) proposed to combine pre-trained models from diverse modalities via contrastive learning by setting image representations as the central modality while fine-tuning all the other models to be aligned with the image encoder. By contrast, BioBRIDGE does not involve the base FMs in training but learns the transformation bridge modules. In addition, the rich structure information in KG is leveraged to relax the central modality assumption and allows for a more controlled cross-modality transformation.

Knowledge Graph Learning. Many knowledge graph embedding learning algorithms have been proposed for KG completion tasks (Han et al., 2018), i.e., given the head node and relation, predict the most probable tail node. These approaches assume a fixed set of nodes and do not handle *inductive* prediction, i.e., prediction for nodes not seen in the training. More recent efforts utilize graph neural networks to handle inductive setup (Teru et al., 2020; Liu et al., 2021), which generate embeddings for new nodes by aggregating its neighbors' embeddings. Nevertheless, they still do not handle isolated new nodes with no link to known nodes. Also, the inherent node properties, e.g., the sequence structure of protein nodes were usually neglected in the encoding. On the contrary, the proposed BioBRIDGE learns from a KG, representing new nodes with base FMs and transforming the embeddings via bridge modules without the need for neighbor graph inputs.

3 METHOD

The study aims to bridge embeddings across multiple modalities supervised by a KG. The overall workflow of BioBRIDGE is illustrated in Figure 2.

3.1 PROBLEM FORMULATION

Knowledge Graph (KG). KG consists of nodes \mathcal{V} and edges \mathcal{E} as $\mathcal{G} = \{\mathcal{V}, \mathcal{E}\}$. A node in the graph, namely $\mathbf{v} = \{\mathbf{x}^v, c^v\}$, constitutes the modality of the node c^v and the node feature \mathbf{x}^v . For example, a protein as a node in the KG is with $c^v = \text{“protein”}$ and \mathbf{x}^v = the protein sequence. An edge $e \in \mathcal{E}$ that associates with two nodes \mathbf{v}_i and \mathbf{v}_j is called a *triple* in the context of KG, as $\mathbf{t}_{ij} = \{\mathbf{v}_i, \mathbf{v}_j, r_{ij}\}$, where r_{ij} indicates the relation between the head and tail nodes. BioBRIDGE uses the structure information from KG, as a triple \mathbf{t} carries the relation between the head and tail nodes coming from two modalities.

Bridge Modalities. We have a set of foundation models (FMs) that were pre-trained on single-modality data. Our target is to bridge the unimodal FMs to fulfill multimodal tasks without fine-tuning the FMs. Specifically, BioBRIDGE bridges arbitrary two samples \mathbf{v}_i and \mathbf{v}_j from two modalities, as $c_i^v \neq c_j^v$. Here, we encode \mathbf{v}_i and \mathbf{v}_j into embeddings: $\mathbf{h}_i = f(\mathbf{x}_i^v)$ and $\mathbf{h}_j = g(\mathbf{x}_j^v)$ where $f(\cdot)$ and $g(\cdot)$ are two FMs hence \mathbf{h}_i and \mathbf{h}_j are in different spaces. We aim to build the trans-

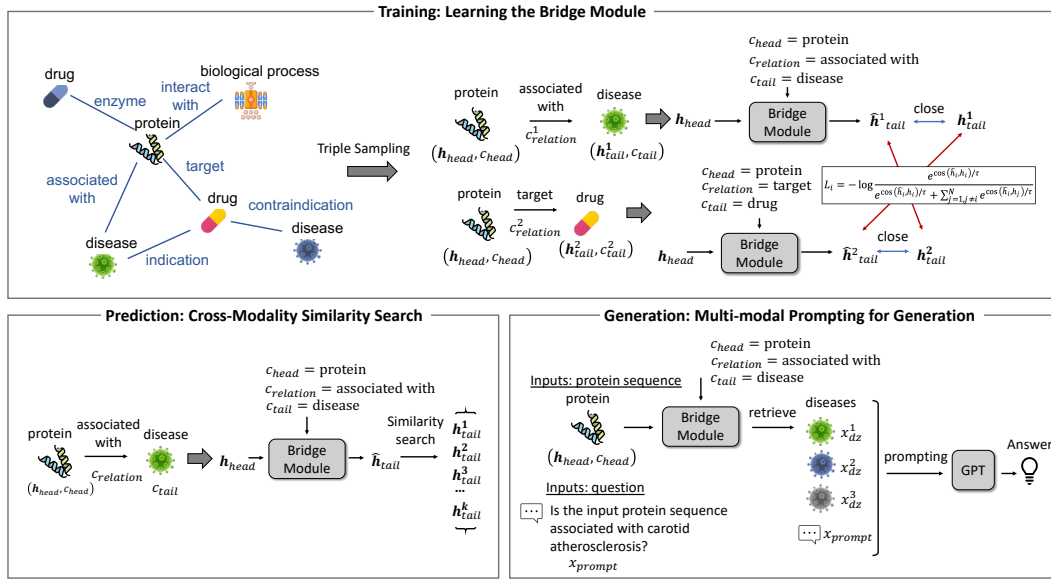


Figure 2: The overall workflow of BioBRIDGE: (1) **top**: we train a bridge module that transforms the head node embedding to the tail node space with contrastive learning. (2) **bottom left**: the trained bridge module enables cross-modal prediction through the similarity search. (3) **bottom right**: The bridge module enables multimodal prompting for retrieval-augmented generation.

formation that projects \mathbf{h}_i to the space of \mathbf{h}_j , as $\hat{\mathbf{h}}_i = \phi(\mathbf{h}_j, c_i^v, c_j^v, r_{ij})$ that considers the modality types of two samples and their relations. As a result, the embedding $\hat{\mathbf{h}}_i$ is aligned with \mathbf{h}_j and can match relevant samples from the modality c_j^v by embedding-based similarity search. We present proof for the existence of a unified bridge module that connects different modalities in Appendix A.

3.2 TRAINING & PREDICTION

Encoding & Transformation. In the training phase, BioBRIDGE samples a triple \mathbf{t}_{ij} that connects \mathbf{v}_i and \mathbf{v}_j from two modalities c_i^v and c_j^v , respectively. We corrupt \mathbf{t}_{ij} by replacing the tail node with others $\{\mathbf{v}_{j'}\}_{j'}$ where $c_{j'}^v = c_j^v$ to build informative negative samples. The bridge module ϕ transforms the head node embedding \mathbf{h}_i to the space of modality c_j^v to yield $\hat{\mathbf{h}}_i$.

Specifically, the raw embedding \mathbf{h} of a sample $\mathbf{v} = \{\mathbf{x}, c\}$ is projected by the modality-specific projection head p as $\mathbf{z} = p_c(\mathbf{h}) \in \mathbb{R}^d$ to ensure all embeddings follow the same dimension. We also treat c_i^v, c_j^v, r_{ij} as categorical variables and generate their embeddings $\mathbf{c}_i, \mathbf{c}_j$, and \mathbf{r}_{ij} , respectively, which all are in dimension of d . The projected head node embedding \mathbf{z}_i is transformed by

$$\hat{\mathbf{h}}_i = \mathbf{z}_i + \psi(\mathbf{z}_i, \mathbf{c}_i, \mathbf{c}_j, \mathbf{r}_{ij}), \quad (1)$$

where $\psi : \mathbb{R}^d \mapsto \mathbb{R}^d$ generates the relation-aware transformation embeddings additive to \mathbf{z}_i .

Loss Function. Based on the encoded tail nodes and the transformed head node, as $\{\hat{\mathbf{h}}_i, \mathbf{z}_j, \underbrace{\mathbf{z}_{j_1}, \dots, \mathbf{z}_{j_M}}_{\text{negative tails}}\}$, we perform contrastive learning with InfoNCE loss (Oord et al., 2018) as

$$\mathcal{L}_{ij} = -\log \frac{\exp(\hat{\mathbf{h}}_i \cdot \mathbf{z}_j / \tau)}{\exp(\hat{\mathbf{h}}_i \cdot \mathbf{z}_j / \tau) + \sum_{j' \neq j}^M \exp(\hat{\mathbf{h}}_i \cdot \mathbf{z}_{j'} / \tau)}, \quad (2)$$

where M is the number of the sampled negative tails; τ is a scalar temperature, and all embeddings are normalized by their ℓ_2 -norm before passing to the loss function. This InfoNCE loss pushes $\hat{\mathbf{h}}_i$ close to the positive tail \mathbf{z}_j , thus bridging two modalities.

Prediction. It is noteworthy that, though triples extracted from KGs are used in the training, BioBRIDGE does not refer to KG for its inference. Consider a task to match $\mathbf{v}_i = \{\mathbf{x}_i^v, c_i^v\}$ to the modality \mathcal{C} , we encode $\mathbf{v}_j, \forall c_j^v \in \mathcal{C}$ by the base FM $g(\cdot)$ and project them into the normalized embeddings $\mathbf{H}_{\mathcal{C}} = \{\mathbf{z}_1, \mathbf{z}_2, \dots, \mathbf{z}_{|\mathcal{C}|}\}$. Then, we encode \mathbf{v}_i with the base FM $f(\cdot)$ and transform it to the embedding space of \mathcal{C} , yielding the normalized $\hat{\mathbf{h}}_i$. We can compare the similarity of $\hat{\mathbf{h}}_i$ with $\mathbf{H}_{\mathcal{C}}$ efficiently through matrix inner product, as $\hat{y} = \mathbf{H}_{\mathcal{C}}^{\top} \hat{\mathbf{h}}_i \in [-1, 1]^{|\mathcal{C}|}$.

3.3 IMPLEMENTATION

Dataset. We draw a subset of PrimeKG (Chandak et al., 2023) to build the training knowledge graph for our method. Specifically, we pick the six main node types from the graph: *Protein*, *Molecule*, *Disease*, *Biological process* (BP), *Molecular function* (MF), and *Cellular component* (CC) without the loss of generality. The statistics of the triples in the training KG are available in Table 8. The exact training set varies depending on the downstream evaluation datasets to avoid data leakage in our experiments. We describe how we curate the training data based on PrimeKG in Appendix B.

Model. We categorize the six types of nodes into three modalities: protein sequence, SMILES strings, and natural language. Technically, we utilized ESM2-3B (Lin et al., 2023) to encode proteins, UniMol (Zhou et al., 2023a) to encode drug molecules, and PubMedBERT (Gu et al., 2021) to encode diseases, biological processes, molecular functions, and cellular components. For a text node, we concatenate its name and definition to form the inputs for PubMedBERT.

While there are many potential options to build the transformation, we deliberately choose a vanilla six-layer transformer model for the bridge module ψ in Eq. 1 to verify the plausibility of the method. In detail, we stack $\mathbf{z}_i, \mathbf{c}_i, \mathbf{c}_j$, and \mathbf{r}_{ij} to build the input $\mathbf{Z} \in \mathbb{R}^{4 \times d}$ for the transformers. We draw the embedding on the first position after the transformer as the output of ψ to add to the input \mathbf{z} .

4 EXPERIMENT: CROSS-MODALITY PREDICTION

In this section, we perform the experiments to test the *prediction* capabilities of BioBRIDGE. Specifically, the prediction tasks can be categorized into:

- **In-domain entity and relation types.** Both the types of the input entity and the input relation are present in the training knowledge graph, where we conducted two series of experiments: cross-modality retrieval tasks (§4.1) and semantic similarity inference (§4.2).
- **In-domain entity and out-of-domain relation types.** We consider the case where the target relations are absent in the training graph, i.e., out domain. We conducted protein-protein interaction prediction for this case (§4.3).
- **Out-of-domain entity and in-domain relation types.** We also conducted experiments for out-domain entities but in-domain relations: cross-species protein-phenotype matching (§4.4).

4.1 CROSS-MODALITY RETRIEVAL TASKS

Setup. Given an input embedding that was encoded by unimodal FMs, our method can transform it to the embedding space of the target modality accounting for their relations. In this sense, we are able to perform cross-modality retrieval by matching the transformed embedding with the candidate samples in the target modality embedding space. To gauge the quality of the transformed embeddings, we compare our methods with a suite of knowledge graph embedding (KGE) methods: TransE (Bordes et al., 2013), TransD (Ji et al., 2015), TransH (Wang et al., 2014), TransR (Lin et al., 2015), ComplEx (Trouillon et al., 2016), DistMult (Yang et al., 2015), and RotatE (Sun et al., 2019), implemented with OpenKE (Han et al., 2018). It is noteworthy that although our method learns from a knowledge graph, it deals with *inductive setup* since it encodes any new node input with unimodal FMs, while these KGE methods assume a fixed set of nodes and require re-training when new nodes are added. BioBRIDGE also differs from inductive graph neural networks that aggregate neighbor nodes to build the embeddings of a new node, while our method does not require the input node with known relations with the existing nodes in the graph.

Dataset & Baseline. We split the raw PrimeKG triples to set up the cross-modality retrieval tasks. For each type of triple, we randomly sample 80%, 10%, and 10% for the train, validation, and test sets, respectively. Then, we separate the test set by triple types, with a special focus on the predictions for: $\{\text{Protein, BP/MF/CC, Interacts with}\}$, $\{\text{Drug, Disease, Indication}\}$, $\{\text{Drug, Protein, Target}\}$, $\{\text{Protein, Disease, Associated with}\}$, $\{\text{Drug, Disease, Contraindication}\}$. The statistics of the train/valid/test data used in this experiment are available in Table 10.

Table 1: Mean reciprocal rank (MRR) on the seven cross-modal prediction tasks. “Drug \nrightarrow Disease” indicates the “contraindication” relation between drug and disease. The best are in bold.

Method	Protein \rightarrow BP	Protein \rightarrow MF	Protein \rightarrow CC	Drug \rightarrow Disease	Protein \rightarrow Drug	Disease \rightarrow Protein	Drug \rightarrow Disease
TransE	0.034	0.046	0.044	0.017	0.033	0.024	0.010
TransR	0.045	0.060	0.048	0.053	0.069	0.028	0.029
TransH	0.044	0.061	0.057	0.026	0.043	0.024	0.014
TransD	0.043	0.059	0.053	0.022	0.049	0.024	0.013
ComplEx	0.084	0.100	0.099	0.042	0.079	0.059	0.048
DistMult	0.054	0.089	0.095	0.025	0.044	0.033	0.047
RotatE	0.079	0.119	0.107	0.150	0.125	0.070	0.076
BioBRIDGE	0.136	0.326	0.319	0.189	0.172	0.084	0.081

Metric. We refer to the KG link prediction literature to use Hit@ K ($K \in \{1, 3, 10\}$), and Mean reciprocal rank (MRR) to evaluate the prediction performance. MRR is the average reciprocal rank of all the positive test triples among the corrupted negative triples. Hit@ K measures the proportion of positive tail entities among the ranked top- K possible candidates. We calculate these metrics on the direction of tail entity prediction.

Result. We show MRR across the seven tasks in Table 1 and the breakdown performances in Tables 11, 12, 13, 14, 15, 16, and 17, respectively. We further report the overall average ranking of all methods across these tasks in Table 9. We found that BioBRIDGE is consistently ranked the best among the KGE methods. The specialized KGE algorithms learn the node and relation embeddings from scratch exclusively based on the KG, while our method builds on pre-trained FMs that already possess rich prior knowledge. As such, BioBRIDGE bridges modalities in a much more data-efficient way. Breaking down into the performance on different tasks, as shown in Table 1, we observed that BioBRIDGE gains a higher margin over baselines on tasks with fewer triples from the KG. For instance, BioBRIDGE is around $3\times$ better than the best baseline for “Protein \rightarrow MF” while is around $1.6\times$ better for “Protein \rightarrow BP”, which signals the benefit of BioBRIDGE in bridging FMs with limited data for multimodal tasks over training a multimodal model from scratch.

4.2 SEMANTIC SIMILARITY INFERENCE

Setup. The objective of this analysis is to evaluate the extent to which the encoded protein embeddings can capture biomolecular functional similarity, i.e., biological process (BP), molecular function (MF), and cellular component (CC). We follow the experimental protocol in (Unsal et al., 2022) that takes the gene ontology (GO) terms annotations of proteins as the target. For our method, we use the protein embeddings transformed to the BP, MF, and CC spaces as the input for evaluation.

Dataset & Baseline. We leverage the test sets released by (Zhou et al., 2023b) where three 500×500 labeled matrices store the pairwise Lin Similarities of the protein associated BP, MF, and CC, respectively. We aggregate these matrices to obtain 1,123 unique protein sequences and remove them from the training knowledge graph to avoid data leakage. We compare our method with the following baselines: MSA Transformer (Rao et al., 2021), ESM-1B (Rives et al., 2021), ProtT5-XL (El-naggar et al., 2021), ESM2-3B (Lin et al., 2023), OntoProtein (Zhang et al., 2022), and KeAP (Zhou et al., 2023b).

Table 2: The comparison on semantic similarity inference across methods. The best are in bold. “Avg” is short for the average of results.

Method	MF	BP	CC	Avg
MSA Transformer	0.38	0.31	0.30	0.33
ProtT5-XL	0.57	0.21	0.40	0.39
ProtBERT	0.41	0.35	0.36	0.37
ESM-1B	0.38	0.42	0.37	0.39
ESM2-3B	0.33	0.42	0.23	0.32
OntoProtein	0.41	0.36	0.36	0.38
KeAP	0.41	0.41	0.40	0.41
BioBRIDGE	0.91	0.80	0.73	0.81

Metric. We compute the pairwise Manhattan Similarities of the encoded protein embeddings as the predictions. The final score is obtained by computing the Spearman’s rank correlation between the predictions and the flattened groundtruth matrix, which is the larger, the better.

Result. We report the results in Table 2, where our method yields a substantial improvement, with around $2\times$ better than the best baseline on average. Across the baselines, we observed the methods augmented by KG, including KeAP and OntoProtein, yield better results than the others, implying that KG connecting proteins and the biological attributes enhance protein representation learning. Nonetheless, BioBRIDGE learns to transform the protein embeddings to the biomolecular functional embedding space, thus aligning protein sequences better with the semantic meaning of functional terms. Also, the involvement of other modalities, like drugs from the KG in training, further enriches the supervision for the transformation model.

4.3 PROTEIN-PROTEIN INTERACTION

Table 3: The F1 scores of the selected methods on the protein-protein interaction task with three datasets. “B+D” is short for the mean of BFS and DFS results. The best results are in bold.

Method	Split ID	SHS27K			SHS148K			STRING		
		BFS	DFS	B+D	BFS	DFS	B+D	BFS	DFS	B+D
KeAP	0	0.695	0.744		0.634	0.831		0.801	0.884	
	1	0.764	0.713		0.626	0.813		0.783	0.886	
	2	0.694	0.790		0.629	0.825		0.765	0.884	
	Avg (Std)	0.718 (0.040)	0.749 (0.039)	0.733	0.630 (0.004)	0.823 (0.009)	0.726	0.783 (0.018)	0.885 (0.001)	0.834
ESM2-3B	0	0.687	0.733		0.637	0.839		0.801	0.880	
	1	0.768	0.725		0.644	0.827		0.781	0.884	
	2	0.690	0.791		0.632	0.819		0.778	0.881	
	Avg (Std)	0.715 (0.046)	0.750 (0.036)	0.732	0.638 (0.006)	0.828 (0.010)	0.733	0.787 (0.013)	0.882 (0.002)	0.834
BioBRIDGE	0	0.704	0.764		0.645	0.840		0.791	0.890	
	1	0.765	0.722		0.638	0.834		0.787	0.891	
	2	0.701	0.778		0.647	0.829		0.769	0.888	
	Avg (Std)	0.723 (0.036)	0.755 (0.029)	0.739	0.643 (0.005)	0.834 (0.005)	0.739	0.782 (0.012)	0.890 (0.002)	0.836

Setup & Metric. We study the protein-protein interaction (PPI) prediction task because it represents the second experiment setup: in-domain entity and out-of-domain relation. The PPI prediction task aims to classify 7 interaction types of a pair of proteins: *reaction*, *binding*, *post-translational modifications (ptmod)*, *activation*, *inhibition*, *catalysis*, and *expression*. Although the *ppi* relation is present in PrimeKG, it only represents the physical interaction (similar to “Binding” in the seven types), while the other six types are out-of-domain.

Following the setup of (Zhang et al., 2022), we extract the protein embeddings with the baseline pre-trained protein models, which serve as the input for a graph neural network model to be trained on the PPI network. Our method uses the protein embeddings transformed to protein space with the relation *ppi*. We report the F1 score for this multi-class classification task.

Dataset & Baseline. Two baselines are selected for comparison: ESM2-3B (Lin et al., 2023) and KeAP (Zhou et al., 2023b). We test them on three PPI datasets: SHS27K (Chen et al., 2019), SHS148K (Chen et al., 2019), and STRING (Lv et al., 2021). Following the setup in (Zhou et al., 2023b), we perform Breadth-First Search (BFS) and Depth-First Search (DFS) to generate two train/validation/test splits, respectively.

Result. From the results in Table 3, we observe that though the results vary across splits, our method shows a consistent improvement over the baselines in most scenarios. It is illustrated that ESM2-3B performs better than the prior state-of-the-art KeAP, which can be attributed to its pre-training on an enormous protein database. BioBRIDGE further enhances the embeddings of ESM2 by injecting the relation “*ppi*”, and then transforms back to the protein space. BioBRIDGE exhibits greater benefit on the datasets with fewer samples like SHS27K as it enriches the protein embedding with the protein-protein interaction ontology information. When the number of training data increases, all methods tend to converge to the same level while the baselines are still inferior to BioBRIDGE.

4.4 CROSS-SPECIES PROTEIN-PHENOTYPE MATCHING

Setup. We propose this novel task to test the capability of BioBRIDGE to handle the cross-modality transformation for out-of-domain entity and in-domain relation. As PrimeKG only contains human proteins, we build a dataset of mouse proteins and the associated mouse phenotypes from the Mouse Genome Informatics (MGI) resource (Eppig et al., 2017), acting as out-of-domain entities. We

elaborate on the curation process of this data in Appendix E. Since the modality “phenotype” is absent in BioBRIDGE’s training data, we transform the encoded mouse protein embeddings to the “disease” space with the relation “associate with”.

Dataset. We build two datasets for 1) matching mouse protein (MG) to mouse phenotype (MP) and 2) matching mouse protein (MG) to human phenotype (HP). The data statistics are available in Table 18. Basically, there are 28 mouse phenotypes to predict for Task 1 and 353 human phenotypes for Task 2, respectively.

Baseline. There is no previous work for this task. We create a dual-encoder model with a protein encoder: ESM2-1B (Lin et al., 2023) and a text encoder: PubMedBERT (Gu et al., 2021). To build the supervised baseline, we perform contrastive learning with the dual-encoder model on the paired mouse protein and phenotype.

Metric. We use a suite of ranking metrics to evaluate the matching performance, including Recall@K, Precision@K, and nDCG@K.

Table 4: The comparison between the zero-shot BioBRIDGE (“0-shot”) and the supervised baseline on the cross-species retrieval tasks. “Diff” indicates the relative improvement of BioBRIDGE over the supervised baseline.

Metric	Task 1: Mouse Protein to Mouse Phenotype			Task 2: Mouse Protein to Human Phenotype			
	Supervised	BioBRIDGE-0-shot	Diff	Metric	Supervised	BioBRIDGE-0-shot	Diff
Rec@1	0.061	0.067	10%	Prec@1	0.001	0.043	3351%
Prec@1	0.360	0.338	-6%	Rec@1	0.001	0.022	3098%
Rec@3	0.145	0.185	28%	Prec@5	0.003	0.022	624%
Prec@3	0.289	0.316	9%	Rec@5	0.011	0.053	393%
Rec@5	0.194	0.278	43%	Rec@10	0.026	0.088	236%
Prec@5	0.233	0.292	25%	Rec@20	0.051	0.168	228%
nDCG@5	0.293	0.350	20%	nDCG@20	0.019	0.082	330%

Result. We report the results in Table 4. This is a challenging task because neither mouse proteins nor mouse/human phenotypes were used in its training data. Despite this, the underlying protein FM underwent comprehensive pre-training on protein sequences across various species. As BioBRIDGE learns to bridge human protein and human diseases, it demonstrates the emergent ability to transform mouse protein from the protein space to mouse phenotype in the text space.

In Task 1, BioBRIDGE showcases a large margin over the supervised baseline that was fine-tuned on the paired mouse protein and phenotype data. This observation underscores the feasibility of transferring BioBRIDGE to a novel domain without further training. In Task 2, the supervised baseline failed to extrapolate to match mouse protein to human phenotype despite being learned on paired mouse proteins and mouse phenotypes. However, BioBRIDGE leverages the prior knowledge of the base FMs on protein and human disease. By projecting protein embeddings into the space of diseases and considering the semantic similarities between many human diseases and phenotypes, the transformed mouse protein embeddings align with human phenotypes through similarity search. This inspiring result hints at the potential for novel bioinformatic analysis based on the bridged FMs enabled via cross-modal matching.

5 CASE STUDY: MULTIMODAL GENERATION

In this section, we show how BioBRIDGE supports a multimodal generation system through cross-modal retrieval. We leverage Galactica-30B (Taylor et al., 2022) that was fine-tuned on instruction datasets as the base generator¹. We prompt Galactica to answer the input question or generate target molecules following the input instruction. The used prompts are in Appendix G.

Multiodal Question & Answer. BioBRIDGE accommodates multimodal input that consists of a molecule SMILES string/protein sequence with an associated question in natural language. In this task, BioBRIDGE serves as a cross-modal retriever to enhance the contexts for Galactica’s response to the input question. Particularly, it retrieves the following: (1) identify the potential protein targets of the input molecule, (2) identify the disease indications for the input molecule, (3)

¹Huggingface: GeorgiaTechResearchInstitute/galactica-30b-evol-instruct-70k

Table 5: Case study of multi-modal Q&A based on BioBRIDGE: Input a molecule/protein and a question, retrieve the relevant diseases and proteins/gene ontology terms, and prompt LLM to answer. The references are drawn for the input molecule/protein-based drug pages from DrugBank.

Input Molecule	Question	Retrieved Disease	Retrieved Protein	Answer	Reference
<chem>CC[C@]1(O)C[C@]2(O)C[C@H]2CN1C</chem> <chem>CC[C@]1(O)C[C@]2(O)C[C@H]2CN1C</chem> <chem>[C@=O]C1=C(OCC=C2CN=C(O)C@H)3</chem> <chem>[C@]4(C)CNC3CC=C[C@]4(O)[CC](C=C@H)45</chem> <chem>[C@=O]H[COC(=O)]C@3(O)C(=O)OC[C@H]2C=1</chem>	What are the associated conditions and pharmacodynamics of this drug?	yolk sac tumor, non-Hodgkin malignant lymphoma, Burkitt lymphoma, malignant sex cord stromal tumor of ovary, B-cell neoplasm, dysgerminoma of ovary, sarccoma, duodenal cancer, malignant Sertoli-Leydig cell tumor of ovary	TUBB8, TUBB8B, TUBB4B, TUBB2B, TUBB4A, TUBB3, TUBA2A, TUBA1C, TUBA3C	[...] the main associated conditions of this small molecule drug could be [cancers of the yolk sac], [...] malignant lymphoma, [...] Hodgkin's disease, [...] acute erythremia, and [...] acute pannyoellosis. The anti-tumor activity of Vincristine is thought to be due primarily to inhibition of mitosis at metaphase through its interaction with tubulin.	Vincristine is a vinca alkaloid used to treat acute leukemia, malignant lymphoma, Hodgkin's disease, acute erythremia, and acute pannyoellosis. The anti-tumor activity of Vincristine is thought to be due primarily to inhibition of mitosis at metaphase through its interaction with tubulin. Ref: DrugBank: DB00541
Input Protein	Question	Retrieved Disease	Retrieved GO Terms	Answer	Reference
<chem>MPTSSSTKKTOLOLEHLLLDLQMLNLGI</chem> <chem>NNYKNPKLTRMLTFKYMPKKATELKHL</chem> <chem>QCLEELKPLKEEVNLNLQSKNPHLPRDLS</chem> <chem>ISININVVLELGSETTTMCEY</chem> <chem>ADETATIVTEFLNRWLTIFS</chem> <chem>QSHISTL</chem>	Describe the pharmacology of this protein-based therapy.	hepatocellular carcinoma, hepatocellular adenoma, adult hepatocellular carcinoma, hepatocellar clear cell carcinoma, liver cancer, undifferentiated carcinoma of liver and intrahepatic biliary tract, nonpapillary renal cell carcinoma, squamous cell carcinoma of liver and intrahepatic biliary tract, familial breast carcinoma, prostate cancer, adenocarcinoma of liver and intrahepatic biliary tract, drug-induced liver injury	positive regulation of cell population proliferation, multicellular organism development, signal transduction, spermatogenesis, cell differentiation, G protein-coupled receptor signaling pathway, negative regulation of cell population proliferation	[...] some possible associated conditions of this protein-based therapy are hepatocellular carcinoma, [...] and intrahepatic biliary tract. The main pharmacodynamics of this therapy could be related to the regulation of cell population proliferation, cell differentiation, and signal transduction, which are all important processes involved in the growth and development of cancer cells. The protein sequence may also have some interactions with metal ions, proteins, and proteases, which could impact its ability to bind to and modulate the activity of other proteins involved in cancer development.	Used to treat renal cell carcinoma. Aldesleukin induces the differentiation of lymphocyte progenitors and stimulation of long-term growth of human interleukin-2 dependent cell lines. Ref: DrugBank: DB00041

identify associated diseases for the input protein, and (4) identify gene ontology terms related to the protein. We choose the drugs from DrugBank that are not in the BioBRIDGE’s training KG. We also involve *investigational* drugs to test if BioBRIDGE can aid in proposing mechanisms-of-action.

Results are shown in Table 5, with more results in Table 19 in the appendix. It demonstrates that BioBRIDGE provides key evidence that prompts Galactica to reach the right answer. For instance, BioBRIDGE can pinpoint a group of tubulin proteins and oncology-related conditions for Vincristine. This process enables Galactica to provide an accurate response, indicating that this drug inhibits the mitosis of cancer cells. In addition, in Table 19, the investigational drug Rimacalib, which has been used in trials studying the treatment of rheumatoid arthritis, is identified by our method to possess immunomodulatory, anti-inflammatory, and anti-arthritic effects. It hence prompts Galactica to reach the answer that this drug may treat diseases such as rheumatoid arthritis.

Table 6: Case study of multi-modal generation based on BioBRIDGE: Input the target condition and the intended mechanism, retrieve the relevant proteins, and prompt LLM to generate the target small molecule drug.

Target Condition	Target Effect	Retrieved Protein	Generated Molecule	Most Similar Drug
malignant lymphoma	The inhibition of mitosis at metaphase of cancer cells via polychemotherapy.	MTHFR, BCL2, TYMS, CAT, CASP8, CSF3, CDKN2A, TP53, CREBBP, SOD2		

Multi-Modal Generation. This task aims to achieve the text-guided generation of small-molecule drugs. We use BioBRIDGE to enrich the context for Galactica by retrieving the target proteins that are possibly associated with the target conditions. To validate the structural integrity of the generated molecules, we utilize RDKit to calculate the Tanimoto distance between the generated SMILES string and all candidate small molecule drugs listed in DrugBank. We then identify the most similar drugs. Results are shown in Table 6 with more in Table 20. We found that (1) BioBRIDGE prompts Galactica to generate valid drug molecules; (2) the generated molecule usually shares similarities with the real drugs that were considered effective for the target condition. For instance, in Table 6, the model-generated drug is most similar to Procarbazine, which is used to treat stage III/IV Hodgkin’s disease in chemotherapy by impeding the division of cancer cells. This implies the generated drug probably fits the proposed target effect and treats lymphoma.

6 CONCLUSION

This paper investigated bridging unimodal biomedical foundation models (FM) for multimodal tasks. We identified that our method BioBRIDGE, can effectively transform the embeddings to

the target modality, considering the types of source modality, target modality, and their relations. We achieved it with great parameter efficiency: only the bridge module needs training while all the base FMs are kept fixed, supervised by the relational information from biomedical knowledge graphs. In experiments, we identified that BioBRIDGE can handle a diverse set of cross-modal prediction tasks by extrapolating to in-domain/out-of-domain entities and relations. And the yielded performances are on par with the supervised specialist models in each task. In addition, we demonstrated how the bridged FMs can support generation tasks with multimodal inputs. In the future, we envision that BioBRIDGE can be extended to connect pre-trained FMs from other domains as long as entities across different modalities can be represented in a KG.

REFERENCES

Viraj Bagal, Rishal Aggarwal, PK Vinod, and U Deva Priyakumar. MolGPT: molecular generation using a transformer-decoder model. *Journal of Chemical Information and Modeling*, 62(9):2064–2076, 2021.

Rishi Bommasani, Drew A Hudson, Ehsan Adeli, Russ Altman, Simran Arora, Sydney von Arx, Michael S Bernstein, Jeannette Bohg, Antoine Bosselut, Emma Brunskill, et al. On the opportunities and risks of foundation models. *arXiv preprint arXiv:2108.07258*, 2021.

Antoine Bordes, Nicolas Usunier, Alberto Garcia-Duran, Jason Weston, and Oksana Yakhnenko. Translating embeddings for modeling multi-relational data. *Advances in Neural Information Processing Systems*, 26, 2013.

Stephen P Boyd and Lieven Vandenberghe. *Convex optimization*. Cambridge university press, 2004.

Tom Brown, Benjamin Mann, Nick Ryder, Melanie Subbiah, Jared D Kaplan, Prafulla Dhariwal, Arvind Neelakantan, Pranav Shyam, Girish Sastry, Amanda Askell, et al. Language models are few-shot learners. *Advances in Neural Information Processing Systems*, 33:1877–1901, 2020.

Payal Chandak, Kexin Huang, and Marinka Zitnik. Building a knowledge graph to enable precision medicine. *Scientific Data*, 10(1):67, 2023. URL <https://doi.org/10.1038/s41597-023-01960-3>.

Muhao Chen, Chelsea J-T Ju, Guangyu Zhou, Xuelu Chen, Tianran Zhang, Kai-Wei Chang, Carlo Zaniolo, and Wei Wang. Multifaceted protein–protein interaction prediction based on siamese residual rcnn. *Bioinformatics*, 35(14):i305–i314, 2019.

John B Conway. *A course in functional analysis*, volume 96. Springer, 2019.

George Cybenko. Approximation by superpositions of a sigmoidal function. *Mathematics of control, signals and systems*, 2(4):303–314, 1989.

Carl Edwards, Tuan Lai, Kevin Ros, Garrett Honke, Kyunghyun Cho, and Heng Ji. Translation between molecules and natural language. In *Conference on Empirical Methods in Natural Language Processing*, 2022.

Ahmed Elnaggar, Michael Heinzinger, Christian Dallago, Ghalia Rehawi, Yu Wang, Llion Jones, Tom Gibbs, Tamas Feher, Christoph Angerer, Martin Steinegger, et al. Prottrans: Toward understanding the language of life through self-supervised learning. *IEEE Transactions on Pattern Analysis and Machine Intelligence*, 44(10):7112–7127, 2021.

Janan T Eppig, Cynthia L Smith, Judith A Blake, Martin Ringwald, James A Kadin, Joel E Richardson, and Carol J Bult. Mouse genome informatics (mgi): resources for mining mouse genetic, genomic, and biological data in support of primary and translational research. *Systems Genetics: Methods and Protocols*, pp. 47–73, 2017.

Benedek Fabian, Thomas Edlich, Hélène Gaspar, Marwin Segler, Joshua Meyers, Marco Fiscato, and Mohamed Ahmed. Molecular representation learning with language models and domain-relevant auxiliary tasks. *arXiv preprint arXiv:2011.13230*, 2020.

Rohit Girdhar, Alaaeldin El-Nouby, Zhuang Liu, Mannat Singh, Kalyan Vasudev Alwala, Armand Joulin, and Ishan Misra. Imagebind: One embedding space to bind them all. In *Proceedings of the IEEE/CVF Conference on Computer Vision and Pattern Recognition*, pp. 15180–15190, 2023.

Vladimir Gligorijević, P Douglas Renfrew, Tomasz Kosciolek, Julia Koehler Leman, Daniel Berenberg, Tommi Vatanen, Chris Chandler, Bryn C Taylor, Ian M Fisk, Hera Vlamakis, et al. Structure-based protein function prediction using graph convolutional networks. *Nature communications*, 12(1):3168, 2021.

Yu Gu, Robert Tinn, Hao Cheng, Michael Lucas, Naoto Usuyama, Xiaodong Liu, Tristan Naumann, Jianfeng Gao, and Hoifung Poon. Domain-specific language model pretraining for biomedical natural language processing. *ACM Transactions on Computing for Healthcare (HEALTH)*, 3(1):1–23, 2021.

Logan Hallee and Jason P Gleghorn. Protein-protein interaction prediction is achievable with large language models. *bioRxiv*, pp. 2023–06, 2023.

Paul R Halmos. *Finite-dimensional vector spaces*. Courier Dover Publications, 2017.

Xu Han, Shulin Cao, Lv Xin, Yankai Lin, Zhiyuan Liu, Maosong Sun, and Juanzi Li. OpenKE: An open toolkit for knowledge embedding. In *Proceedings of EMNLP*, 2018.

Kurt Hornik. Approximation capabilities of multilayer feedforward networks. *Neural networks*, 4(2):251–257, 1991.

Kexin Huang, Cao Xiao, Lucas M Glass, and Jimeng Sun. MolTrans: molecular interaction transformer for drug–target interaction prediction. *Bioinformatics*, 37(6):830–836, 2021.

Vassilis N. Ioannidis, Xiang Song, Saurav Manchanda, Mufei Li, Xiaoqin Pan, Da Zheng, Xia Ning, Xiangxiang Zeng, and George Karypis. Drkg - drug repurposing knowledge graph for covid-19. <https://github.com/gnn4dr/DRKG/>, 2020.

Guoliang Ji, Shizhu He, Liheng Xu, Kang Liu, and Jun Zhao. Knowledge graph embedding via dynamic mapping matrix. In *Proceedings of ACL*, pp. 687–696, 2015.

John Jumper, Richard Evans, Alexander Pritzel, Tim Green, Michael Figurnov, Olaf Ronneberger, Kathryn Tunyasuvunakool, Russ Bates, Augustin Žídek, Anna Potapenko, et al. Highly accurate protein structure prediction with alphafold. *Nature*, 596(7873):583–589, 2021.

Yogesh Kalakoti, Shashank Yadav, and Durai Sundar. Transdtt: transformer-based language models for estimating dtis and building a drug recommendation workflow. *ACS omega*, 7(3):2706–2717, 2022.

Alexander Kirillov, Eric Mintun, Nikhila Ravi, Hanzi Mao, Chloe Rolland, Laura Gustafson, Tete Xiao, Spencer Whitehead, Alexander C Berg, Wan-Yen Lo, et al. Segment anything. *arXiv preprint arXiv:2304.02643*, 2023.

Yankai Lin, Zhiyuan Liu, Maosong Sun, Yang Liu, and Xuan Zhu. Learning entity and relation embeddings for knowledge graph completion. In *Proceedings of the AAAI Conference on Artificial Intelligence*, volume 29, 2015.

Zeming Lin, Halil Akin, Roshan Rao, Brian Hie, Zhongkai Zhu, Wenting Lu, Nikita Smetanin, Robert Verkuil, Ori Kabeli, Yaniv Shmueli, et al. Evolutionary-scale prediction of atomic-level protein structure with a language model. *Science*, 379(6637):1123–1130, 2023.

Shengchao Liu, Yutao Zhu, Jiarui Lu, Zhao Xu, Weili Nie, Anthony Gitter, Chaowei Xiao, Jian Tang, Hongyu Guo, and Anima Anandkumar. A text-guided protein design framework. *arXiv preprint arXiv:2302.04611*, 2023.

Shuwen Liu, Bernardo Grau, Ian Horrocks, and Egor Kostylev. Indigo: Gnn-based inductive knowledge graph completion using pair-wise encoding. *Advances in Neural Information Processing Systems*, 34:2034–2045, 2021.

Guofeng Lv, Zhiqiang Hu, Yanguang Bi, and Shaoting Zhang. Learning unknown from correlations: graph neural network for inter-novel-protein interaction prediction. *arXiv preprint arXiv:2105.06709*, 2021.

Ali Madani, Ben Krause, Eric R Greene, Subu Subramanian, Benjamin P Mohr, James M Holton, Jose Luis Olmos Jr, Caiming Xiong, Zachary Z Sun, Richard Socher, et al. Large language models generate functional protein sequences across diverse families. *Nature Biotechnology*, pp. 1–8, 2023.

Aaron van den Oord, Yazhe Li, and Oriol Vinyals. Representation learning with contrastive predictive coding. In *NeurIPS*, 2018.

Jianing Qiu, Lin Li, Jiankai Sun, Jiachuan Peng, Peilun Shi, Ruiyang Zhang, Yinzhaodong, Kyle Lam, Frank P-W Lo, Bo Xiao, et al. Large ai models in health informatics: Applications, challenges, and the future. *arXiv preprint arXiv:2303.11568*, 2023.

Alec Radford, Jong Wook Kim, Chris Hallacy, Aditya Ramesh, Gabriel Goh, Sandhini Agarwal, Girish Sastry, Amanda Askell, Pamela Mishkin, Jack Clark, et al. Learning transferable visual models from natural language supervision. In *International conference on machine learning*, pp. 8748–8763. PMLR, 2021.

Roshan M Rao, Jason Liu, Robert Verkuil, Joshua Meier, John Canny, Pieter Abbeel, Tom Sercu, and Alexander Rives. Msa transformer. In *International Conference on Machine Learning*, pp. 8844–8856. PMLR, 2021.

Alexander Rives, Joshua Meier, Tom Sercu, Siddharth Goyal, Zeming Lin, Jason Liu, Demi Guo, Myle Ott, C Lawrence Zitnick, Jerry Ma, et al. Biological structure and function emerge from scaling unsupervised learning to 250 million protein sequences. *Proceedings of the National Academy of Sciences*, 118(15):e2016239118, 2021.

Samuel Sledzieski, Rohit Singh, Lenore Cowen, and Bonnie Berger. Adapting protein language models for rapid dti prediction. *bioRxiv*, pp. 2022–11, 2022.

Teague Sterling and John J Irwin. Zinc 15-ligand discovery for everyone. *Journal of chemical information and modeling*, 55(11):2324–2337, 2015.

Gilbert Strang. *Linear algebra and its applications*. 2012.

Zhiqing Sun, Zhi-Hong Deng, Jian-Yun Nie, and Jian Tang. Rotate: Knowledge graph embedding by relational rotation in complex space. *arXiv preprint arXiv:1902.10197*, 2019.

Ross Taylor, Marcin Kardas, Guillem Cucurull, Thomas Scialom, Anthony Hartshorn, Elvis Saravia, Andrew Poulton, Viktor Kerkez, and Robert Stojnic. Galactica: A large language model for science. *arXiv preprint arXiv:2211.09085*, 2022.

Komal Teru, Etienne Denis, and Will Hamilton. Inductive relation prediction by subgraph reasoning. In *International Conference on Machine Learning*, pp. 9448–9457. PMLR, 2020.

Théo Trouillon, Johannes Welbl, Sebastian Riedel, Éric Gaussier, and Guillaume Bouchard. Complex embeddings for simple link prediction. In *International Conference on Machine Learning*, pp. 2071–2080. PMLR, 2016.

Serbulent Unsal, Heval Atas, Muammer Albayrak, Kemal Turhan, Aybar C Acar, and Tunca Doğan. Learning functional properties of proteins with language models. *Nature Machine Intelligence*, 4(3):227–245, 2022.

Sheng Wang, Yuzhi Guo, Yuhong Wang, Hongmao Sun, and Junzhou Huang. SMILES-BERT: large scale unsupervised pre-training for molecular property prediction. In *Proceedings of the 10th ACM international conference on bioinformatics, computational biology and health informatics*, pp. 429–436, 2019a.

Yanbin Wang, Zhu-Hong You, Shan Yang, Xiao Li, Tong-Hai Jiang, and Xi Zhou. A high efficient biological language model for predicting protein–protein interactions. *Cells*, 8(2):122, 2019b.

Zhen Wang, Jianwen Zhang, Jianlin Feng, and Zheng Chen. Knowledge graph embedding by translating on hyperplanes. In *Proceedings of the AAAI Conference on Artificial Intelligence*, volume 28, 2014.

Zichen Wang, Steven A Combs, Ryan Brand, Miguel Romero Calvo, Panpan Xu, George Price, Nataliya Golovach, Emmanuel O Salawu, Colby J Wise, Sri Priya Ponnappalli, et al. Lm-gvp: an extensible sequence and structure informed deep learning framework for protein property prediction. *Scientific reports*, 12(1):6832, 2022a.

Zifeng Wang, Zhenbang Wu, Dinesh Agarwal, and Jimeng Sun. Medclip: Contrastive learning from unpaired medical images and text. In *Proceedings of the 2022 Conference on Empirical Methods in Natural Language Processing*, pp. 3876–3887, 2022b.

Minghao Xu, Xinyu Yuan, Santiago Miret, and Jian Tang. Protst: Multi-modality learning of protein sequences and biomedical texts. In *ICML*, 2023.

Bishan Yang, Scott Wen-tau Yih, Xiaodong He, Jianfeng Gao, and Li Deng. Embedding entities and relations for learning and inference in knowledge bases. In *Proceedings of the International Conference on Learning Representations (ICLR) 2015*, 2015.

Ningyu Zhang, Zhen Bi, Xiaozhuan Liang, Siyuan Cheng, Haosen Hong, Shumin Deng, Qiang Zhang, Jiazhang Lian, and Huajun Chen. Ontoprotein: Protein pretraining with gene ontology embedding. In *International Conference on Learning Representations*, 2022.

Gengmo Zhou, Zhifeng Gao, Qiankun Ding, Hang Zheng, Hongteng Xu, Zhewei Wei, Linfeng Zhang, and Guolin Ke. Uni-Mol: A universal 3d molecular representation learning framework. In *The Eleventh International Conference on Learning Representations*, 2023a.

Hong-Yu Zhou, Yunxiang Fu, Zhicheng Zhang, Bian Cheng, and Yizhou Yu. Protein representation learning via knowledge enhanced primary structure reasoning. In *The Eleventh International Conference on Learning Representations*, 2023b.

A PROVING EXISTENCE OF BRIDGE MODULE AND LEARNABILITY

This section aims to show the existence of a bridge module, followed by its learnability. Given our setup of unimodal FMs, we will show the existence of transformation modules that can take us from any modality's output space to another under certain assumptions. We will proceed to first state our assumptions and then the statement, followed by the proof for the statement.

Assumptions 1 (Assumptions on the neural networks and Knowledge Graph).

1. Let $K \in \mathbb{Z}^+$ be the total number of modalities and let M_1, \dots, M_K denote the K neural networks trained on the different modalities whose parameters are now frozen.
2. For every neural network $M_k : \Omega_k \rightarrow S_k$, $d > 0$, $k \in \{1, \dots, K\}$, $S_k \subseteq \mathbb{R}^d$, Ω_k denotes the input space/ domain and the output space S_k for every neural network is a linear subspace of \mathbb{R}^d . Specifically, we will assume the dimension of every subspace is the same.
3. Let $\mathcal{G} = (\mathcal{V}, \mathcal{E})$ denote the knowledge graph where \mathcal{V} is the set of nodes and \mathcal{E} is the set of edges. Each node $v \in \mathcal{V}$ belongs to one of the K modalities.
4. Every $e \in \mathcal{E}$ of the knowledge graph which connects two nodes $v_i, v_j \in \mathcal{V}$ has an associated relation type $r_{ij} \in \mathcal{R}$.

Theorem 1 (Existence of a Bridge Module). *For any given pair of nodes $v_i, v_j \in \mathcal{V}$ of modality types $k_{v_i}, k_{v_j} \in \{1, \dots, K\}$ and with representations given by their appropriate neural networks $s_{v_i} \in S_{k_{v_i}}, s_{v_j} \in S_{k_{v_j}}$, which are connected by relation type $r_{ij} \in \mathcal{R}$, there exists a bridge module $B : \mathbb{R}^d \times \{1, \dots, K\} \times \{1, \dots, K\} \times \mathcal{R} \rightarrow \mathbb{R}^d$ such that $B : (s_{v_i}, k_{v_i}, k_{v_j}, r_{ij}) \mapsto s_{v_j}$*

Proof. At a very high level, a direct consequence of the Hahn-Banach Theorem (Conway, 2019) can be used to see that given a Euclidean space and given two compact, convex subsets of that Euclidean space, there exists a continuous function mapping between them (given that there is a linear functional that separates them). Given our assumption that our subspaces are linear and therefore convex, as well as the assumption of continuity of neural networks, we can quickly assert the existence of transformations between the spaces.

Here, however, we will go into the details and show a simple proof using linear algebra. We will use a multi-step approach to prove the existence of the bridge module. Firstly, we will look at expressibility in terms of linear subspaces and then introduce conditional transformations based on relation types. Subsequently, we will look at the compositionality and aggregation of paths (as we are dealing with knowledge graphs) for the bridge module. We will specifically look at linear subspaces here, but similar arguments can also be established for convex hull-like spaces or other spaces that have an established geometry.

First, we look at the linear mapping between linear subspaces. Given any two linear subspaces S_x, S_y , a linear transformation between the two is one which maps points in S_x to S_y i.e. $T_{xy} : S_x \rightarrow S_y$ - and this can always be represented using a matrix A_{xy} as $T_{xy}(p) = A_{xy} \cdot p$, $p \in S_x$. The existence of such a transformation is guaranteed by the rank nullity theorem (Strang, 2012) without any loss of information (as the dimensions of the subspaces are taken to be the same by construction).

Next, any relation in $r_{ij} \in \mathcal{R}$ can be represented as a vector, i.e., a relation embedding $r(r_{ij}) \in \mathbb{R}^p$, $p > 0$ and the transformation T between subspaces can be a function over the matrix A_{xy} as well as $r(r_{ij})$ i.e. $A_{xy}^a = f(A_{xy}, r(r_{ij}))$ and the conditional transformation (relation dependent) of any point $p \in S_x$ via relation r_{ij} is now given as $T_{xy}^{r_{ij}}(p) = A_{xy}^{r_{ij}} \cdot p$. Such a formulation also allows us to directly model compositionality of transformations (due to the properties of matrices) as given two transformations T_{xy}, T_{yz} between $S_x \rightarrow S_y \rightarrow S_z$, a composition $T_{yz} \circ T_{xy}$ (given by $A_{yz}^{r_{jk}} \cdot A_{xy}^{r_{ij}}$ in matrix notation) captures a transformation from S_x to S_z . Given that we are dealing with linear subspaces and transformations, these compositions are always defined (Strang, 2012).

Next, we look at the aggregation of multiple paths - since we are dealing with KGs, there can be multiple paths between any two nodes. In such cases, the transformation between any two subspaces can then be obtained as a weighted combination of the paths, i.e., $A_{agg} = \sum_{i=1}^N w_i A_i$ such that $\sum_{i=1}^N w_i = 1$ where w_i is the weight associated with a path and A gives the transformation matrix between the spaces. When all $w_i > 0$, this forms a convex combination and ensures that the aggregated transformation is still within the space by the original transformations (Boyd & Vandenberghe, 2004) and therefore confirms the existence of a unified bridge module. \square

Now, given the existence of the above transformations as defined by the KG, the convergence of sequences of linear transformations (Halmos, 2017), the universality of neural networks (Hornik, 1991; Cybenko, 1989) and the continuity of the unimodal FM’s ensure that such conditional transformations (given by relation types) can be approximated when appropriate loss functions are employed via SGD.

B ESTABLISHING TRAINING DATA BASED ON PRIMEKG

Table 7: The statistics of nodes and edges of the raw PrimeKG data and the processed KG for training BioBRIDGE. “Original”: the original PrimeKG; “Processed”: the processed KG; “Dropped”: how many samples are dropped in the processing.

Nodes		Original	Processed	Dropped	Percent dropped
Modality					
biological process	28,642	27,478	1,164		4.06%
protein	27,671	19,162	8,509		30.75%
disease	17,080	17,080	0		0.00%
molecular function	11,169	10,966	203		1.82%
drug	7,957	6,948	1,009		12.68%
cellular component	4,176	4,013	163		3.90%
Summation	96,695	85,647	11,048		11.43%
Edges		Original	Processed	Dropped	Percent Dropped
Relation type					
drug_drug	2,672,628	2,241,466	431,162		16.13%
protein_protein	642,150	629,208	12,942		2.02%
bioprocess_protein	289,610	272,642	16,968		5.86%
cellcomp_protein	166,804	149,504	17,300		10.37%
disease_protein	160,822	155,924	4,898		3.05%
molfunc_protein	139,060	133,522	5,538		3.98%
bioprocess_bioprocess	105,772	99,630	6,142		5.81%
disease_disease	64,388	64,388	0		0.00%
contraindication	61,350	60,130	1,220		1.99%
drug_protein	51,306	47,614	3,692		7.20%
molfunc_molfunc	27,148	26,436	712		2.62%
indication	18,776	17,578	1,198		6.38%
cellcomp_cellcomp	9,690	9,200	490		5.06%
off-label use	5,136	4,998	138		2.69%
Summation	4,414,640	3,912,240	502,400		11.38%

The raw PrimeKG provides a bind of biomedical entities from a widespread of sources. However, it does not provide the associated properties for all the entities, e.g., the sequence structure of the proteins. To train BioBRIDGE, we try to link the entities to the external knowledge bases and filter out those without the required property. The statistics of raw KG and the processed are available in Table 7. We describe the data curation process for each type of entities as the following.

Protein Data. There are 27,671 proteins in total in the original PrimeKG. We try to match the provided NCBI gene ID of the proteins to the UniProtKB/Swiss-Prot sequence database, via the uniprot id-mapping tool <https://www.uniprot.org/id-mapping>. We were able to retrieve 27,478 protein sequences that are matched with the gene ID.

We delve deeper into the unmapped proteins and find most are non-protein-coding genes (pseudo-genes, rRNA, ncRNA genes), which are genes unable to produce proteins. It is hence reasonable to ignore them for protein-centric tasks.

Drug Data. There are 7,957 drugs in the original PrimeKG. We try to match the offered DrugBank ID to the database <https://go.drugbank.com/drugs>. We dropped drugs without SMILES strings to obtain a total of 6,948 drugs.

Gene Ontology Terms. Biological process, molecular function, and cellular component are represented by all gene ontology (GO) terms. We leveraged AmiGO for searching the detailed descriptions of the GO terms through their IDs <https://amigo.geneontology.org/amigo/>

[search/ontology](#). We were able to retrieve the features of the most GO terms then kept 27,478 BP, 10,966 MF, and 4,013 MF, in the training data.

Disease. The descriptions of those diseases are provided by the raw PrimeKG data so we are able to keep all 17,080 diseases for training.

C DATA STATISTICS OF THE KNOWLEDGE GRAPH

Table 8: The data statistics of the training knowledge graph drawn from PrimeKG.

Head Node	Tail Node	Relation	Number	
protein	protein	ppi	642,150	
	biological process	interacts with	144,805	
	cellular component	interacts with	83,402	
	molecular function	interacts with	69,530	
	disease	associated with	80,411	
	drug	target	16,380	
		enzyme	5,317	
		transporter	3,092	
drug		carrier	864	
	drug	synergistic interaction	2,672,628	
		contraindication	30,675	
		indication	9,388	
		off-label use	2,568	
		target	16,380	
		enzyme	5,317	
		transporter	3,092	
disease	protein	carrier	864	
		disease	parent-child	64,388
		gene/protein	associated with	80,411
		drug	contraindication	30,675
			indication	9,388
			off-label use	2,568

D CROSS-MODALITY RETRIEVAL TASKS

Table 9: The mean and standard deviation (in parenthesis) of the ranks of all compared methods across the seven cross-modality retrieval tasks. Lower rank is better. Best are in bold.

Method	Rank-MRR (↓)	Rank-Hits@10 (↓)	Rank-Hits@3 (↓)	Rank-Hits@1 (↓)
TransE	7.71 (0.00)	7.71 (0.00)	7.43 (0.52)	5.00 (0.00)
TransR	5.00 (1.41)	4.57 (1.63)	5.14 (1.47)	5.00 (0.00)
TransH	5.86 (0.82)	5.71 (0.55)	6.00 (0.41)	5.00 (0.00)
TransD	6.71 (0.84)	6.57 (0.82)	6.57 (0.82)	5.00 (0.00)
ComplEx	3.00 (0.63)	3.43 (0.55)	3.00 (0.63)	2.86 (0.63)
DistMult	4.57 (1.03)	5.00 (1.67)	4.00 (1.79)	3.14 (0.89)
RotatE	2.14 (0.41)	2.00 (0.00)	2.43 (0.84)	2.86 (0.98)
BioBRIDGE	1.00 (0.00)	1.00 (0.00)	1.00 (0.00)	1.00 (0.00)

Table 10: The data statistics of the train/valid/test splits used in cross-modality retrieval tasks.

Triple Type	# Head Node	# Tail Node	# Train Triple	# Valid Triple	# Test Triple
Protein - Interacts with - BP	16,808	12,047	111,649	11,620	13,052
Protein - Interacts with - MF	17,289	4,284	55,252	5,438	6,071
Protein - Interacts with - CC	17,211	1,684	61,471	6,250	7,031
Protein - Associated with - Disease	8,548	5,566	63,869	6,659	7,434
Drug - Indication - Disease	1,592	1,279	7,290	704	795
Drug - Contraindiation - Disease	1,217	1,181	24,423	2,676	2,966
Drug - Target - Protein	5,074	2,620	12,952	920	1,055

Table 11: Cross-modality prediction performance for triple type: “Protein - Interacts with - BP”.

Method	MRR	Hit@10	Hit@3	Hit@1	MRR Rank	Hit@10 Rank	Hit@3 Rank	Hit@1 Rank
TransE	0.034	0.097	0.020	0.000	8	8	8	5
TransR	0.045	0.136	0.023	0.000	5	4	5	5
TransH	0.044	0.129	0.023	0.000	6	6	6	5
TransD	0.043	0.125	0.020	0.000	7	7	7	5
ComplEx	0.084	0.218	0.067	0.020	2	3	2	2
DistMult	0.054	0.132	0.045	0.013	4	5	4	3
RotatE	0.079	0.239	0.057	0.012	3	2	3	4
BioBRIDGE	0.136	0.282	0.146	0.066	1	1	1	1

Table 12: Cross-modality prediction performance for triple type: “Protein - Interacts with - MF”.

Method	MRR	Hit@10	Hit@3	Hit@1	MRR Rank	Hit@10 Rank	Hit@3 Rank	Hit@1 Rank
TransE	0.046	0.143	0.030	0.000	8	8	8	5
TransR	0.060	0.196	0.041	0.000	6	6	5	5
TransH	0.061	0.199	0.040	0.000	5	5	6	5
TransD	0.059	0.185	0.039	0.000	7	7	7	5
ComplEx	0.100	0.289	0.080	0.020	3	3	3	4
DistMult	0.089	0.203	0.080	0.033	4	4	3	2
RotatE	0.119	0.360	0.103	0.021	2	2	2	3
BioBRIDGE	0.326	0.653	0.382	0.177	1	1	1	1

Table 13: Cross-modality prediction performance for triple type: “Protein - interacts with - CC”.

Method	MRR	Hit@10	Hit@3	Hit@1	MRR Rank	Hit@10 Rank	Hit@3 Rank	Hit@1 Rank
TransE	0.044	0.133	0.026	0.000	8	8	7	5
TransR	0.048	0.142	0.023	0.000	7	7	8	5
TransH	0.057	0.176	0.029	0.000	5	5	5	5
TransD	0.053	0.162	0.026	0.000	6	6	6	5
ComplEx	0.099	0.267	0.081	0.023	3	3	3	3
DistMult	0.095	0.212	0.092	0.034	4	4	2	2
RotatE	0.107	0.330	0.079	0.018	2	2	4	4
BioBRIDGE	0.319	0.676	0.373	0.160	1	1	1	1

Table 14: Cross-modality prediction performance for triple type: “Drug - Indication - Disease”.

Method	MRR	Hit@10	Hit@3	Hit@1	MRR Rank	Hit@10 Rank	Hit@3 Rank	Hit@1 Rank
TransE	0.017	0.057	0.006	0.000	8	8	8	5
TransR	0.053	0.152	0.019	0.000	3	3	4	5
TransH	0.026	0.074	0.015	0.000	5	5	6	5
TransD	0.022	0.064	0.018	0.000	7	6	5	5
ComplEx	0.042	0.084	0.028	0.010	4	4	3	3
DistMult	0.025	0.063	0.010	0.004	6	7	7	4
RotatE	0.150	0.357	0.150	0.054	2	2	2	2
BioBRIDGE	0.189	0.380	0.176	0.071	1	1	1	1

Table 15: Cross-modality prediction performance for triple type: “Protein - Target - Drug”.

Method	MRR	Hit@10	Hit@3	Hit@1	MRR Rank	Hit@10 Rank	Hit@3 Rank	Hit@1 Rank
TransE	0.033	0.086	0.016	0.000	8	8	8	5
TransR	0.069	0.204	0.058	0.000	4	3	4	5
TransH	0.043	0.127	0.018	0.000	7	6	6	5
TransD	0.049	0.150	0.018	0.000	5	5	6	5
ComplEx	0.079	0.184	0.075	0.021	3	4	3	3
DistMult	0.044	0.104	0.035	0.008	6	7	5	4
RotatE	0.125	0.258	0.131	0.051	2	2	2	2
BioBRIDGE	0.172	0.299	0.181	0.107	1	1	1	1

Table 16: Cross-modality prediction performance for triple type: “Disease - Associated with - Protein”.

Method	MRR	Hit@10	Hit@3	Hit@1	MRR Rank	Hit@10 Rank	Hit@3 Rank	Hit@1 Rank
TransE	0.010	0.015	0.002	0.000	8	8	7	5
TransR	0.029	0.066	0.007	0.000	5	5	5	5
TransH	0.014	0.020	0.003	0.000	6	6	6	5
TransD	0.013	0.018	0.002	0.000	7	7	7	5
ComplEx	0.048	0.106	0.031	0.010	3	4	4	3
DistMult	0.047	0.113	0.035	0.010	4	3	3	3
RotatE	0.076	0.172	0.059	0.021	2	2	2	2
BioBRIDGE	0.081	0.184	0.071	0.025	1	1	1	1

Table 17: Cross-modality prediction performance for triple type: “Drug - Contraindication - Disease”.

Method	MRR	Hit@10	Hit@3	Hit@1	MRR Rank	Hit@10 Rank	Hit@3 Rank	Hit@1 Rank
TransE	0.010	0.015	0.002	0.000	8	8	7	5
TransR	0.029	0.066	0.007	0.000	5	5	5	5
TransH	0.014	0.020	0.003	0.000	6	6	6	5
TransD	0.013	0.018	0.002	0.000	7	7	7	5
ComplEx	0.048	0.106	0.031	0.010	3	4	4	3
DistMult	0.047	0.113	0.035	0.010	4	3	3	3
RotatE	0.076	0.172	0.059	0.021	2	2	2	2
BioBRIDGE	0.081	0.184	0.071	0.025	1	1	1	1

Table 18: The statistics of the built cross-species retrieval dataset.

Mouse Protein - Mouse Phenotype		Mouse Protein - Human Phenotype	
Item	Train	Item	Test
MGI	6,069	6,068	MGI
MPI	28	28	HPO
Pairs	38,705	37,937	Pairs
Mean MPI	6.38	6.26	Mean HPO

E MOUSE PROTEIN AND PHENOTYPE DATASET

We retrieved the paired mouse protein and phenotype data from https://www.informatics.jax.org/downloads/reports/HMD_HumanPhenotype.rpt, yielding a total of 29,686 paired mouse protein ID (MGI), human protein ID, and mouse phenotype ID (MPI), namely data1. We then retrieved the detailed descriptions of mouse phenotypes from https://www.informatics.jax.org/downloads/reports/MPheno_OBO.ontology, yielding 14,201 MPI and their definition, namely data2.

To obtain the exact sequence structure of mouse proteins, we called UniProt <https://www.uniprot.org/id-mapping> mapping system, choosing “MGI” under “Organism-specific databases” as the source database, “UniproKB/Swiss-Prot” as the target database. This process maps MGI to the corresponding protein sequences, namely data3.

We only keep MGI that is with protein sequence referring to data3 from data1. Also, we only keep MGI in data1 that is linked to more than one MPI. Finally, we conduct a filter from data1 to keep human proteins that are in the PrimeKG data and link to more than one human protein. The obtained dataset then has 14,024 MGI, 14,200 MPI, 1,582 Human Proteins, and 3,279 Human Phenotypes in total.

F CASE STUDY: MULTIMODAL Q&A

Table 19: Additional case studies of multi-modal Q&A based on BioBRIDGE: Input a molecule and a question, retrieve the relevant diseases and proteins, and prompt LLM to answer. The references are drawn for the input molecule-based drug pages from DrugBank.

Input Molecule	Question	Retrieved Disease	Retrieved Protein	Answer	Reference
[C][C@H](C1=NOC(=N)C(N)2CCOC2)C1=C1=CC=C(C(F)=C1)C1=CC=CC=C1	What are the associated conditions and pharmacodynamics of this drug?	osteoporosis postmenopausal osteoporosis psoriasis allergic contact dermatitis atopic eczema rheumatoid arthritis osteonecrosis allergic asthma systemic lupus erythematosus (disease) congestive heart failure	MAPK14 CDK2 MAPK1 MAPK8 MAPK3 EP300 MAPK9 CREBBP GSK3B MAPK10	The associated diseases and the proteins this molecule targets suggest that this small molecule drug may have immunomodulatory, anti-inflammatory, and analgesic properties. The drug may inhibit the activity of MAPK14, which plays a role in the production of pro-inflammatory cytokines. This inhibition may help reduce inflammation in conditions such as psoriasis, allergic contact dermatitis, atopic eczema, rheumatoid arthritis, and allergic asthma. The drug may also inhibit the activity of CDK2, which is involved in the regulation of the cell cycle and proliferation of immune cells. This inhibition may help suppress the immune system and reduce inflammation in systemic lupus erythematosus (disease). Additionally, the drug may inhibit the activity of other MAPK family members such as [...], which are involved in the regulation of immune responses and inflammation. The drug may also activate EP300 and CREBBP, which are transcriptional co-activators that regulate the expression of genes involved in anti-inflammatory responses. Overall, the main pharmacodynamics of this small molecule drug may be immunomodulatory, anti-inflammatory, and anti-arthritis effects, making it a potential treatment option for various conditions such as psoriasis, allergic contact dermatitis, atopic eczema	Rimacalib has been used in trials studying the treatment of Rheumatoid Arthritis (RA). [DrugBank: DB12571]
[N C@H](C=O)N [C-CH2]C2C C(F)2C [C@H]C1CN C12CC3CC (CC(O)C3)C1C2	What are the associated conditions and pharmacodynamics of this drug?	diabetes mellitus (disease) type 2 diabetes mellitus coronary artery disease bipolar disorder bipolar II disorder bipolar depression bipolar I disorder obesity disorder dysthymic disorder monogenic obesity neurotic disorder diabetic ketoacidosis	DPP4 F2 FAP F9 PRSS2 PLAT F10 ACE DPB6 PRSS1	Based on the associated diseases and the proteins this molecule targets, the main possible associated conditions of this small molecule drug are type 2 diabetes, obesity, coronary artery disease, neurotic disorder, dysthymic disorder, monogenic obesity, diabetic ketoacidosis, and bipolar disorders. The main pharmacodynamics of this small molecule drug are its inhibitory effects on dipeptidyl peptidase 4 (DPP4) and fibroblast activation protein alpha (FAP), which may help reduce the risk of type 2 diabetes and obesity. The drug may also have some effects on the cardiovascular system, potentially reducing the risk of coronary artery disease and other cardiovascular-related disorders. Additionally, the drug may have some anti-inflammatory effects through its inhibition of FAP, which may contribute to its efficacy in managing some neurotic and mood disorders.	Saxagliptin is a dipeptidyl peptidase-4 (DPP-4) inhibitor antidiabetic for the treatment of type 2 diabetes. [DrugBank: DB06335]
CN/ [CN CCSC1=CC=C [CN(C C)O1)= C N+ O-)=O	Which diseases can this molecule treat and why?	conjunctivitis (disease) duodenal ulcer (disease) pulmonary embolism (disease) gastroenteritis chronic duodenal ileus peptic ulcer disease intralobar congenital pulmonary sequestration Echinococcus infectous disease trachoma lower respiratory tract disease	NOS2 NOS3 GSTP1 GSTA2 GSTA1 GSTM2 GSTM1 GSTA5 GSTM4 PTGS2	Based on the target proteins and associated diseases listed, the main possible associated conditions of this small molecule drug are: 1. Conjunctivitis (disease) 2. Pulmonary embolism (disease) 3. Gastroenteritis 4. Chronic duodenal ileus 5. Peptic ulcer disease 6. Echinococcus infectous disease	Ramitidine is a histamine H2-antagonist used to treat duodenal ulcers, Zollinger-Ellison syndrome, gastric ulcers, GERD, and erosive esophagitis. [DrugBank: DB00863]
[H]C@[[H]2OC3=C (OC)C=CC4=C3[C@H] 11CCN(C C@H)[H]) C4 C@H 1(H)] C=C[C@H]2O	What are the associated conditions and pharmacodynamics of this drug?	vasomotor rhinitis allergic rhinitis seasonal allergic rhinitis perennial allergic rhinitis common cold atopic conjunctivitis nasal polyps palpebral conjunctivitis giant papillary conjunctivitis vernal conjunctivitis pharyngitis angioedema allergic asthma	OPRM1 OPRK1 OPRD1 OPRL1 HTR2C HTR2A DRD2 CHRM2 HTR2B DRD3	The main pharmacodynamics of this small molecule drug would depend on its interaction with the target proteins. As it targets nitric oxide synthase 2 and 3, it may have vasodilation and anti-inflammatory effects. As it targets glutathione S-transferase pi 1, alpha 2, alpha 1, mu 2, mu 1, alpha 5, mu 4, and prostaglandin-endoperoxide synthase 2, it may have antioxidant and anti-inflammatory effects. Additionally, as it is a small molecule drug, it may have a good ability to cross cell membranes and reach its targets quickly.	Cocaine is utilized as a central analgesic, sedative, hypnotic, antinociceptive, and anesthetic agent, and is also recommended in certain diseases with incessant coughing. [Drugbank: DB00318]
CN C@[[H]2OC3=C [C@H]2CC[C@H]3 C2C1C C	What are the associated conditions and pharmacodynamics of this drug?	alcohol dependence substance abuse substance dependence alcohol abuse heroin dependence cannabis dependence cocaine abuse cocaine dependence	SLC6A3 HTR1A CHRM2 SLC6A2 CHRM3 SLC6A4 DRD2 CHRM4 CHRM5 HTR1B	Based on the associated diseases and the proteins this molecule targets, the main possible associated conditions of this small molecule drug are pain, asthma, and allergic reactions. The main pharmacodynamics of this small molecule drug are its activity as an opioid receptor agonist, which can regulate the release of neurotransmitters involved in pain, mood, respiration, and immune function. It can also have anti-inflammatory and anti-allergic effects, although the exact mechanisms are not fully understood. Therefore, this drug may be effective in treating pain and asthma, as well as allergic conditions such as vasomotor rhinitis, allergic rhinitis, and allergic asthma.	Dexmecamylamine has been used in trials studying the basic science and treatment of Patients, Depression, Drug Abuse, Pharmacokinetics, and Renal Impairment, among others. [DrugBank: DB11807]
[O Al]O O OS(=O) (=O)OC C@H O [C@ @H]O C@ 2 (COS-O)=O O Al (O)O [O Al]O O OS(=O)=O O Al O C@ @H [O Al]O [C@ @H]2OS(=O)=O O Al [O O]O C@H OS(=O)=O O Al O C@ @H OS(=O) [O O]O Al O O [C@ @H] OS(=O)=O O Al O O	What are the associated conditions and pharmacodynamics of this drug?	esophagitis (disease) gallbladder disease gallbladder disease 2 gallbladder disease 3 cancer of liver perforated disease kidney disease diarrheal disease gastroesophageal reflux disease asthma pyrourer inherited hemoglobinopathy acute myocardial infarction hemoglobinopathy acquired hemoglobinopathy	TF SOD2 TGFB1 IL6 LTF MMP2 TFRC ALB VEGFA CAT	The small molecule drug described targets multiple proteins involved in the regulation of various neurotransmitters and their receptor pathways. The associated diseases and conditions that this drug could possibly address include drug and alcohol dependence, substance abuse and dependence, and related disorders such as anxiety and depression. The main pharmacodynamics of this drug involve the modulation of the neurotransmitter systems of the brain and peripheral nervous system, which are involved in the regulation of mood, conditional responses, reward-seeking behaviors, and cognitive function. The specific actions of this drug on each of the target proteins are not explicitly stated in the given information, but based on the known functions of these proteins, this drug could potentially regulate the release, reuptake, and signaling of these neurotransmitters, leading to the alleviation of symptoms associated with the associated diseases and conditions.	Dexmecamylamine has been used in trials studying the basic science and treatment of Patients, Depression, Drug Abuse, Pharmacokinetics, and Renal Impairment, among others. [DrugBank: DB11807]
				Based on the information provided, it appears that the small molecule drug may have anti-inflammatory and antioxidant effects as it targets several proteins involved in inflammation and oxidative stress, including interleukin 6, superoxide dismutase 2, transforming growth factor beta 1, and vascular endothelial growth factor A. In terms of associated conditions, the drug may be effective in treating diseases that involve inflammation and oxidative stress, such as cirrhosis of the liver, peptic ulcer disease, diarrheal disease, and kidney disease. It may also have potential in treating gastroesophageal reflux disease and gallbladder diseases, which are also associated with inflammation and oxidative stress. However, it's important to note that these are just speculative associations based on the limited information provided.	Sucralfate aids in the healing of duodenal ulcers, relieving painful inflammation by creating a protective mechanical barrier between the lining of the skin and the underlying tissue and damaging substances 2. In addition, sucralfate acts to increase levels of growth factors locally, and also causes an increase in prostaglandins which are important in the healing of the mucous (lining) of the gastrointestinal tract 2. [DrugBank: DB00364]

Table 20: Case study of multi-modal generation based on BioBRIDGE: Input the target condition and the intended mechanism, retrieve the relevant proteins, and prompt LLM to generate the target small molecule drug.

G CASE STUDY: PROMPT

Listing 1: The prompt for prompting language models to answer user questions takes the drug molecule structure as the input.

```
prompt = """Drug molecule structure: [START_I_SMILES] {smiles}
           [END_I_SMILES]

Target proteins:
{protein_names}

Associated diseases:
{disease_names}

Consider the associated diseases and the proteins this molecule targets,
{input_question}
"""

```

Listing 2: The prompt for prompting language models to generate drug molecule guided by user inputs in natural language.

```
prompt = """The drug may be targeting the proteins:
{protein_names}

{text_guidance}

Generate the most possible SMILES structure of this drug.
"""

```
